Cerebellar heterogeneity and its impact on PET data quantification of 5-HT receptor radioligands.

Ganz M, Feng L, Hansen HD, Beliveau V, Svarer C, Knudsen GM, Greve DN.

First published online: January 11 2017

by Sage Journals for the International Society for Cerebral Blood Flow and Metabolism

in the Journal of Cerebral Blood Flow and Metabolism: J Cereb Blood Flow Metab. 2017 Sep;37(9):3243-3252.

doi: 10.1177/0271678X16686092

Cerebellar heterogeneity and its impact on PET data quantification of 5-HT receptor radioligands

Melanie Ganz[1], Ling Feng[1], Hanne Demant Hansen[1], Vincent Beliveau[1,2], Claus Svarer[1], Gitte Moos Knudsen[1,2], Douglas N. Greve[3,4]

[1]Neurobiology Research Unit and Center for Integrated Molecular Brain Imaging, Rigshospitalet, Copenhagen, Denmark
[2]Faculty of Health and Medical Sciences, University of Copenhagen, Copenhagen, Denmark
[3]Athinoula A. Martinos Center for Biomedical Imaging, Department of Radiology, Massachusetts General Hospital, Boston, MA, USA
[4] Harvard Medical School, Boston, MA, USA

Corresponding author:
Gitte Moos Knudsen, Neurobiology Research Unit, 28 Juliane Maries Vej, Rigshospitalet, building 6931, 2100 Copenhagen, Denmark.

Funding:
Collection of data that was included in the study was supported by the Lundbeck Foundation Center of Excellence Cimbi [R90-A7722]. Melanie Ganz' research was supported by the Carlsberg foundation [2013-01-0502] and National Institutes of Health (NIH) [5R21EB018964-02]. Hanne Demant Hansen was supported by the Lundbeck Foundation Center of Excellence Cimbi [R90-A7722]. Ling Feng's research was financially supported by the European Union's Seventh Framework Programme (FP7/2007-2013) under grant agreement n° HEALTH-F2-2011-278850 (INMiND). Vincent Beliveau's research was supported by the Danish Council for Independent Research - Medical Sciences [4183-00627] and the Research Council of Rigshospitalet [R84 A3300]. Doug Greve was supported by National Institutes of Health (NIH) [1R21EB018964-01 and S10RR023043].

Abstract

In the quantification of positron emission tomography (PET) radiotracer binding, a very commonly used method is the reference tissue model (RTM). RTM necessitates a proper reference region and cerebellum is the most commonly used for G-protein coupled receptors, however, the cerebellum is a heterogenous brain region and can be divided into subregions. We investigated regional differences in uptake within the grey matter of the cerebellar hemispheres (CH) and the cerebellar vermis (CV) for five PET radioligands targeting the serotonin system. Furthermore, we looked into the impact of choosing either CH, CV or CV+CH as a reference region when quantifying the binding of the five radioligands.

The PET and MR images are all part of the Cimbi database: 5-HT_{1A}R ([^{11}C]CUMI,n=8), 5-HT_{1B}R ([^{11}C]AZ10419369,n=36), 5-HT_{2A}R ([^{11}C]Cimbi-36,n=29), 5-HT_4R ([^{11}C]SB207145,n=59), and 5-HTT ([^{11}C]DASB,n=100). We employed the software packages SUIT and FreeSurfer to delineate CV and CH and quantified mean standardized uptake values (SUV) as well as non-displaceable neocortical binding potential (BP_{ND}). Statistical difference was assessed within subjects and with paired nonparametric two-sided Wilcoxon signed rank tests.

We demonstrated radioligand specific regional differences in cerebellar uptake between CV and CH for four out of the five radioligands. These differences may be ascribed to differences in concentration of the receptor or transporter in question in CV vs. CH, could reflect off-target binding of the radioligands or differences in the non-displaceable binding in the two regions. Our data highlight the importance of validating each radioligand carefully for defining the optimal reference region.

Keywords

Reference region, cerebellum, serotonin (5-HT) receptors, vermis

1 Introduction

Positron emission tomography (PET) allows for the visualization of the density of neurotransmitter receptors and transporters and is one of the key tools for in vivo imaging. PET is used to quantify neuroreceptor density in the human brain using binding potential as a metric. Binding potential is defined as the concentration of a radioligand specifically bound to a target receptor divided by a reference concentration. In general, three different reference concentrations can be used: (1) free (non-protein bound) radioligand concentration in plasma, (2) total (free plus protein-bound) radioligand concentration in plasma and (3) non-displaceable radioligand (i.e. the non-specifically bound radioligand plus the free ligand in tissue). Each of these references represents a balance between interpretability and convenience.

The first two methods require measuring the radioligand concentration in plasma which necessitates arterial blood measurements (venous blood sampling is possible in some cases). However, the invasiveness of a required arterial line hampers its feasibility in a clinical setting. Furthermore, the measurements of the parent (non-metabolized) radioligand in plasma can be challenging and labor-intensive. The non-displaceable method, on the other hand, does not require blood sampling at all, but merely requires a region that is free of target of interest. This region then represents the non-displaceable concentration and can be determined using the measured PET image. There have been several methods developed to compute the binding potential using a reference region; collectively, these are known as reference tissue models (RTM)[1]. The binding potential computed relative to the non-displaceable concentration is referred to as BP_{ND}.

A RTM, however, necessitates a proper reference region. RTMs have three basic assumptions: the reference region is devoid of the target of interest; the non-displaceable binding, V_{ND}, is the same for both the target region and the reference region; and the blood volume contribution is negligible in both the reference and target regions. The quantification will be biased if these assumptions are violated, and the bias may not be a simple scaling factor[2]. For G-protein coupled receptors, such as those in the serotonin and dopamine systems, the cerebellum is often used as reference region as it is assumed to be receptor free. However, studies of serotonin receptors suggest that some subregions of the cerebellum may not be receptor free; properly identifying these subregions may be important when using cerebellum as a reference region[3,4].

The cerebellum can be subdivided into subregions that may vary in terms of their suitability as reference tissue. A subregion of specific interest in serotonin imaging is the cerebellar vermis (CV). It can be defined in different ways, but is mostly used to indicate the "midline" of the cerebellum[5]. Previous studies have reported increased 5-HT_{1A}Rs in CV compared to the cerebellar hemispheres (CH) in both healthy volunteers[3] and in schizophrenic patients[6]. But the results are controversial, since another group could not confirm the earlier post-mortem findings of increased 5-HT_{1A}R binding in CV in patients with schizophrenia in vivo[7].

In order to shed more light on the use of cerebellum as a reference region and specifically the properties of CV, we utilized the Center for Integrated Molecular Brain Imaging (Cimbi) database [8] to investigate regional differences in binding within the grey matter of CH and CV for five different PET radioligands targeting the serotonin system.

2 Materials and Methods

2.1 Participants

The Cimbi database[8] established normative data for the 5-HT_{1A} [9], 5-HT_{1B}[10], 5-HT_{2A}[11]and the 5-HT_4[12] receptors as well as the 5-HTT[13]. We selected data of healthy controls for five radioligands targeting these receptors and transporter. All subjects were scanned on a Siemens high resolution research tomography (HRRT) PET scanner. Corresponding T1-weighted structural magnetic resonance (MR) scans were acquired on four different Siemens MR scanners with standard parameters. Demographic details about the participants can be seen in Table 1 of the supplementary material. All procedures followed were in accordance with the ethical standards of the responsible committees on human experimentation (institutional and national) and with the Declaration of Helsinki 1975, as revised in 2008. Informed consent was obtained from all patients for being included in the study.

2.2 Positron Emission Tomography and Structural Magnetic Resonance Imaging

The PET and MR images used in our analysis are all part of the Cimbi database. In detail the following PET scans were available for analysis: 5-HT_{1A}R ([^{11}C]CUMI, n=8), 5-HT_{1B}R ([^{11}C]AZ10419369, n=36), 5-HT_{2A}R ([^{11}C]Cimbi-36, n=29), 5-HT_4R ([^{11}C]SB207145, n=59), and 5-HTT ([^{11}C]DASB, n=100).

PET list-mode data were acquired with a Siemens HRRT scanner operating in 3D-acquisition mode, with an approximate in-plane resolution of 2 mm. PET frames were reconstructed using a 3D-OSEM-PSF algorithm [14–16]. Scan time and frame length was tracer dependent, see [8] for details. Realignment of dynamic PET frames was performed using AIR 5.2.5[17] to account for within-scan motion. A rigid realignment transform was evaluated for individual frames believed to have sufficient count statistics. Frames were smoothed using a 10 mm Gaussian filter, and voxels less than 80% of the maximum intensity were discarded. The remaining voxels were used to evaluate the rigid transformation to the reference frame using least-squares intensity rescaling as the cost-function. The original frames were finally realigned by applying the rigid transformation. Frames with lower count statistics were aligned accordingly to the first or last realigned frame. Details of the realignment procedure can be found in Table 2 of the supplementary material.

Structural MRIs were acquired on four different Siemens scanners - two Siemens Verio, a Siemens Prisma and a Siemens Trio. The detailed acquisition parameters can be found in the supplementary material. The structural MRI data were analyzed with FreeSurfer (v5.3)[18] to define tissue types and regions, including cortical grey matter. The individual cortical surfaces were reconstructed using the structural MRI corrected for gradient non-linearity. PET-MR co-registration was estimated using boundary-based registration[19] between the time-weighted sum of the PET time activity curves (TACs) and the structural MRI[20]. FreeSurfer was used to define a segmentation of the cerebellum in grey and white matter (see Figure 1). Additionally, we employed the software package SUIT 2.7[21] to segment the cerebellum into sub regions – namely CH and CV (also see Figure 1). The CH was defined as those voxels in the cerebellum that were not labelled as CV. Finally, grey matter cerebellar labels were further refined by limiting them to the intersection of the FreeSurfer labels with the cerebellum labelled by SUIT. This removes peripheral overlabeling sometimes present in the FreeSurfer as well as the SUIT segmentation.

[insert Figure 1.]

2.3 Analysis

We computed the volume of CV, CH and the white matter in the cerebellar hemispheres by counting the number of voxels in each segmented region and dividing by the size of the voxels in the segmentation. For each subject we quantified a measure of radioligand uptake in CV, CH and CH+CV. The mean standard uptake values (SUV) weighted by the frame length was used as a measure of brain uptake, where SUV is defined as the TAC in the region-of-interest divided by injected dose per kg bodyweight (g/ml)[22].

Additionally, we calculated the neocortical BP_{ND} with the simplified reference tissue model (SRTM)[23], where we used CV, CH or CH+CV as reference region, respectively. Regional TACs were used for the quantification. We are aware of the fact that we are violating the assumptions for SRTM if CV has specific binding and additionally is a small region, but since SRTM is commonly used to quantify non-displaceable binding potential, we want to assess the bias that including CV yields when using SRTM.

Statistical difference was assessed within subjects and with paired nonparametric two-sided Wilcoxon signed rank tests using Matlab (Mathworks Inc., MA, vers. R2013a).

3 Results

In our segmentations the cerebellum as a whole had on average a volume of 147±15 cm^3 in our population of 232 young healthy adults (for age ranges see Table 1 of the supplementary material). Looking at the subregions, CV had an average volume of 6±0.7 cm^3, CH had an average volume of 110±12 cm^3 and the white matter of the cerebellar hemispheres was 31±4 cm^3. Hence, CV comprises about 4% of the cerebellum, CH covers 75%, and the white matter covers 21% of the whole cerebellum in our dataset.

Regarding differences in cerebellar uptake and neocortical binding potential based on different reference region definitions, we give an overview of the results in Table 3 of the supplementary material.

Figure 2 shows the percentage difference between CV and CH in mean SUV defined as ($meanSUV_{CV}$-$meanSUV_{CH}$)/ $meanSUV_{CH}$. A significant difference between CH and CV was found for [^{11}C]CUMI, [^{11}C]AZ10419369, [^{11}C]Cimbi-36 and [^{11}C]DASB (Table 1 (a)). We found no significant difference in uptake between CH and CV for [^{11}C]SB207145. The difference in uptake between CV and CH ranges from 7- 20% for [^{11}C]CUMI, 0-17% for [^{11}C]AZ10419369, 0-8% for [^{11}C]Cimbi-36 and 0-16% for [^{11}C]DASB.
And even though CV is much smaller than CH and covers only about 4% of the whole cerebellum, this statistical difference persists when we compare CH vs. CH+CV (Table 1 (a)).

[insert Figure 2.]

Next, we calculated neocortical BP_{ND} using different reference regions, where we used CH, CV or CH+CV as reference. The mean and standard deviation as well as the range of neocortical BP_{ND} are given in Table 4 of the supplementary material. Figure 3 shows the percentage difference in neocortical BP_{ND} defined as ($BP_{ND,CV}$ - $BP_{ND,CH}$)/ $BP_{ND,CH}$. A significant difference in BP_{ND} was found for [^{11}C]CUMI-101, [^{11}C]AZ10419369 and [^{11}C]DASB (Table 1 (b)). We found no significant difference in BP_{ND} for [^{11}C]Cimbi-36 and [^{11}C]SB207145. When only using the CV as reference region, the effect size on the neocortical BP_{ND} is large: The difference in BP_{ND} between CV and CH ranges from 11-32% for [^{11}C]CUMI, from 0-40% for [^{11}C]AZ10419369, from 0-15% for [^{11}C]Cimbi-36 and from 0-50% for [^{11}C]DASB.

[insert Figure 3.]

Figure 4 shows the percentage difference ($BP_{ND,CV+CH}$ - $BP_{ND,CH}$)/ $BP_{ND,CH}$, i.e. when CV and CH is combined to a single reference region (CV+CH). As for the mean SUV we also found the same statistical differences when we compare the neocortical BP_{ND} based on CH vs. CH+CV (Table 1 (b)). The differences are though much smaller and range from 0-2% for [^{11}C]CUMI-101, from 0-2% for [^{11}C]AZ10419369, from 0-1% for [^{11}C]Cimbi-36 and from 0-3% for [^{11}C]DASB.

[insert Figure 4.]

4 Discussion

Our measurement of global cerebellar size fits well with other MR based studies, e.g. [24] which reported a total cerebellar volume of 141±13 cm^3 in a population of 97 young (age 33.7 ± 13.6 years) healthy adults.

Regarding the differences in uptake measured by mean SUV the results from the literature vary from receptor to receptor. Looking at the 5-HT_{1A}R there has been in vitro evidence of limited 5-HT_{1A}R binding in CV[36]. In vivo experiments have reported an individual with exceptionally high accumulation of [^{11}C]WAY-100635 in the cerebellum, which was most marked in cerebellar cortical grey matter and vermis [25], as well as significantly reduced cerebellar grey matter (~ 30%) binding after a challenge with pindolol, a 5-HT_{1A}R antagonist [26]. This aligns with our findings where [^{11}C]CUMI-101 had higher uptake in the CV than CH.

For the 5-HT_{1B} receptor sparse evidence exists. In vitro results using [^{3}H]GR125743 report that binding in general was low in the cerebellum[27], but higher in an inner layer of cerebellar cortex close to the white matter[28]. To our knowledge there have been no in vivo reports of higher binding in CH versus CV. In [29] the authors report a low concentration of [^{11}C]AZ10419369 binding in cerebellar cortex and state that BP_{ND} values obtained with kinetic compartment analysis and RTM using the cerebellar cortex as reference region were well correlated. Furthermore, a blocking study in humans using [^{11}C]AZ10419369 and AZD3783[30] states that there is no evident reduction in radioactivity in the cerebellum meaning some subjects showed reduced binding in the cerebellum after blocking whereas others did not. Our results using [^{11}C]AZ10419369 indicate the same as the autoradiography data and point to a slightly higher uptake in CH compared to CV.

The literature for the 5-HT_{2A}R is more cohesive on the subject of cerebellar binding. Several in vitro studies report low to very low 5-HT_{2A}R densities over the different layers of cerebellar cortex using [^{3}H]MDL100907[27] and ketanserin[31]; they concluded that the cerebellum is virtually devoid of 5-HT_{2A}Rs (with [^{3}H]MDL100907)[32]. Furthermore, there is also an in vivo study that reports no detectable cerebellar binding to 5-HT_{2A}Rs using [^{18}F]Altanserin[33]. Our SUV results contradict the literature and indicate a higher uptake in CV compared to CH using [^{11}C]Cimbi-36; however, there was no significant difference in BP_{ND} when using CH or CV as reference. The reason that the SUV

but not the BP_{ND} is significantly different between CV and CH might stem from the sensitivity of the SUV which is a more direct and model-free measure. A higher uptake in CV could be explained by the fact that Cimbi-36 is less selective for the 5-HT_{2A}R compared to MDL100907: The ratio of 5-HT_{2A}R/5-HT_{2C}R selectivity for [^{11}C]Cimbi-36 is 15 [34] while it is 142 for MDL100907[35]. Thus, the binding of Cimbi-36 in CV could be due to the off-target binding to the 5-HT_{2C}R. On the other hand the presence of 5-HT_{2C}R in the cerebellum is unconfirmed[36].

Three in vitro studies of 5-HT_4R report low and inconsistently detectable levels in cerebellar cortex with [^{3}H]GR113808[37] or find no evidence for specific binding in the cerebellum with [^{125}I]SB207710[27 38]. The autoradiography findings are in line with our results, where we see no difference in cerebellar subregion uptake for [^{11}C]SB207145.

Finally, there exists conflicting evidence for the binding of 5-HTT receptors in cerebellum. One in vitro study reported that concentration of the 5-HTT protein in both cerebellar cortex and white matter is very low[39]. However, Varnäs at al. reported that [^{3}H]Citalopram binding was concentrated in a band that probably corresponded to the Purkinje cell layer[27]. Parsey et al. found specific 5-HTT binding to be much higher in CV (8.4 fmol/mg) compared with CH (1.25 fmol/mg), and cerebellar white matter (0.23 fmol/mg) using [^{3}H]cyanoimipramine[40]. Conversely, one in vivo studies states the opposite and reports a negligible level of specific binding with [^{11}C]McN 5652[41]. Our results seem to support the findings in [40] in that we see higher uptake of [^{11}C]DASB in CV compared to CH.

We also evaluated the influence of using different cerebellar sub regions as reference region for neocortical RTM. The differences in neocortical binding when using CH or CH+CV are in general small. The largest differences were found when using CV as reference. Since CV is a very small region, the signal is very noisy and hence the RTM is affected by this higher noise level. Furthermore, the protein/lipid composition may differ between CV and CH and hence the kinetics of CV as reference region could be unsuitable. The influence of including or excluding CV from the reference region when calculating cortical BP_{ND} is small, yielding a difference in cortical BP_{ND} below 5% for all tracers.

Because we find significant differences in uptake and neocortical BP_{ND} for several 5-HT receptors, we hypothesize that there is 1) a difference in the actual receptor densities in the two areas, 2) that there exists off-target binding of the radioligand or 3) that there is a difference in the non-displaceable binding in the two tissue types. Fortunately, we can also show that the differences between including or excluding CV when calculating neocortical BP_{ND} are small. They can, however, bias results and since the bias is different for each patient and each tracer[2] this can be a confounding factor especially for small size PET studies.

Furthermore, the bias from including or excluding CV is possibly larger in disease groups, because the distribution and quantity of receptors can be different in disease groups compared to controls and hence influences group studies to a greater degree. For example, a recent article covering contradictory results regarding 5-HT_{1A} receptors in major depressive disorder [42] highlighted the importance of choosing the right reference region for determining the BP_{ND}. Hence, the authors also recommended using common methodological methods for quantification of BP_{ND} in order to make studies comparable across multiple centres. This includes a common and robust way to define a reference region from MR.

Based on our results we recommend to use CH as reference region and exclude CV. But for the 5-HT_{1B} receptor where we have found a slightly higher uptake of [^{11}C]AZ10419369 in CH compared to CV, we recommend to use CH as reference region with caution. We cannot recommend to only use CV as reference region, since our BP_{ND} calculations vary strongly due to the small size and possibly different tissue composition of the region.

Limitations of our study are that we cannot address age effects, since our population consists of young healthy individuals. Our findings cannot be generalized to clinical populations, because differences in the receptor distribution within the cerebellum has been found in patient populations such as schizophrenics and major depression disorder[6,43].

4.1 Conclusion

We demonstrated radioligand specific regional differences in cerebellar uptake, of relevance for its use as a reference region in PET imaging. These differences may be ascribed to differences in concentration of the receptor or transporter in question in CV vs. CH, could reflect off-target binding of the radioligands or differences in the non-displaceable binding in the two tissue types. There was evidence from post-mortem autoradiography and in vivo studies of the presence of 5-HT_{1A}Rs in CV and we observed a significantly higher [^{11}C]CUMI-101 uptake in the CV compared to CH. We also found significantly higher uptake of [^{11}C]AZ10419369 in CH compared to CV, which is consistent with an autoradiographic study showing presence of 5-HT_{1B}Rs in CH. Our results on 5-HT_{2A} receptor binding in CV were contrary to the in vitro as well as in vivo literature, but this may be explained by the binding of [^{11}C]Cimbi-36 to the 5-HT_{2C}R. With regard to 5-HT_4 receptor binding in the cerebellum, our results agreed with the literature. Finally, we found a higher uptake of [^{11}C]DASB in CV compared to CH; this agrees with [40] but has not been confirmed in other studies.

Besides regional differences in cerebellar uptake we also evaluated the influence of using different cerebellar regions for neocortical RTM. While we observe large difference when using CV alone as reference region, which is most likely due to the unsuitability of SRTM for this region, the influence of including or excluding CV from the reference region is small and yields a difference in cortical BP_{ND} below 5% for all tracers.

In conclusion, our data highlighted the importance of validating each radioligand carefully with regard to the suitability of including or excluding CV in the reference region definition.

5 Acknowledgements

The Cimbi Database and associated biobank were supported by the Lundbeck Foundation R90-A7722 through its grant to establish Cimbi, by the Danish Research Council 09-063598, and by Rigshospitalet. The authors thank all colleagues within the Cimbi Consortium who as part of the extensive Cimbi project (http://www.cimbi.org) have contributed directly or indirectly with data to the database

6 Author contribution statement

MG and LF jointly developed the concept and performed the data analysis. HDH contributed to the literature review. VB performed the preprocessing of the data and investigated approaches to delineate vermis. CS and DG contributed greatly to the discussion of the method and its assumptions. GMK strongly contributed to the discussion of the application of the method and its clinical relevance. MG wrote the first draft and searched for relevant articles. LF, HDH, VB, CS, GMK and DG reviewed the choice of references, tables, and figures and edited the initial draft and every subsequent draft. All authors approved the final manuscript.

7 Disclosure/Conflict of Interest

Melanie Ganz , Hanne Demant Hansen, Ling Feng, Vincent Beliveau, Claus Svarer and Douglas Greve declare that they have no conflict of interest. Gitte Moos Knudsen has been an invited lecturer at Pfizer A/S, worked as a consultant and received grants from H. Lundbeck A/S and is a stock holder of Novo Nordisk/Novozymes. Furthermore, she is on the board of directors of the BrainPrize and Elsass foundation and the advisory board of the Kristian Jebsen Foundation and has authored for FADL and served as editor for Elsevier (IJNP).

8 References:

1. Zanderigo F, Ogden RT, Parsey R V. Reference region approaches in PET: a comparative study on multiple radioligands. *J Cereb Blood Flow Metab* 2013; 33: 888–97.
2. Salinas C a, Searle GE, Gunn RN. The simplified reference tissue model: model assumption violations and their impact on binding potential. *J Cereb Blood Flow Metab* 2014; 35: 1–8.
3. Parsey R V, Arango V, Olvet DM, et al. Regional heterogeneity of 5-HT1A receptors in human cerebellum as assessed by positron emission tomography. *J Cereb Blood Flow Metab* 2005; 25: 785–93.
4. Parsey R V., Oquendo MA, Ogden RT, et al. Altered serotonin 1A binding in major depression: A [carbonyl-C-11] WAY100635 positron emission tomography study. *Biol Psychiatry* 2006; 59: 106–113.
5. Schmahmann JD, Doyon J, McDonald D, et al. Three-dimensional MRI atlas of the human

cerebellum in proportional stereotaxic space. *Neuroimage* 1999; 10: 233–60.

6. Slater P, Doyle C a., Deakin JFW. Abnormal persistence of cerebellar serotonin-1A receptors in schizophrenia suggests failure to regress in neonates. *J Neural Transm* 1998; 105: 305–315.

7. Bantick RA, Montgomery AJ, Bench CJ, et al. A positron emission tomography study of the 5-HT1A receptor in schizophrenia and during clozapine treatment. *J Psychopharmacol* 2004; 18: 346–54.

8. Knudsen GM, Jensen PS, Erritzoe D, et al. The Center for Integrated Molecular Brain Imaging (Cimbi) Database. *Neuroimage* 2015; 1–7.

9. Pinborg LH, Feng L, Haahr ME, et al. No change in [11C]CUMI-101 binding to 5-HT 1A receptors after intravenous citalopram in human. *Synapse* 2012; 66: 880–884.

10. da Cunha-Bang S, Hjordt L V, Perfalk E, et al. Serotonin 1B receptor binding is associated with trait anger and level of psychopathy in violent offenders. *Biol Psychiatry*. Epub ahead of print 2016. DOI: 10.1016/j.biopsych.2016.02.030.

11. Ettrup A, da Cunha-Bang S, McMahon B, et al. Serotonin 2A receptor agonist binding in the human brain with [^{11}C]Cimbi-36. *J Cereb Blood Flow Metab* 2014; 34: 1188–96.

12. Madsen K, Haahr MT, Marner L, et al. Age and sex effects on 5-HT4 receptors in the human brain: a [(11)C]SB207145 PET study. *J Cereb Blood Flow Metab* 2011; 31: 1475–81.

13. Erritzoe D, Holst K, Frokjaer VG, et al. A nonlinear relationship between cerebral serotonin transporter and 5-HT(2A) receptor binding: an in vivo molecular imaging study in humans. *J Neurosci* 2010; 30: 3391–7.

14. Comtat C, Sureau FC, Sibomana M, et al. Image based resolution modeling for the HRRT OSEM reconstructions software. *IEEE Nucl Sci Symp Conf Rec* 2008; 4120–4123.

15. Hong IK, Chung ST, Kim HK, et al. Ultra fast symmetry and SIMD-based projection-backprojection (SSP) algorithm for 3-D PET image reconstruction. *IEEE Trans Med Imaging* 2007; 26: 789–803.

16. Sureau FC, Reader AJ, Comtat C, et al. Impact of image-space resolution modeling for studies with the high-resolution research tomograph. *J Nucl Med* 2008; 49: 1000–1008.

17. Woods RP, Cherry SR, Mazziotta JC. Rapid automated algorithm for aligning and reslicing PET images. *J Comput Assist Tomogr* 1992; 16: 620–633.

18. Fischl B. FreeSurfer. *Neuroimage* 2012; 62: 774–81.

19. Greve DN, Fischl B. Accurate and robust brain image alignment using boundary-based

registration. *Neuroimage* 2009; 48: 63–72.

20. Greve DN, Svarer C, Fisher PM, et al. Cortical surface-based analysis reduces bias and variance in kinetic modeling of brain PET data. *Neuroimage* 2013; 92C: 225–236.

21. Diedrichsen J, Balsters JH, Flavell J, et al. A probabilistic MR atlas of the human cerebellum. *Neuroimage* 2009; 46: 39–46.

22. Thie JA. Understanding the standardized uptake value, its methods, and implications for usage. *J Nucl Med* 2004; 45: 1431–4.

23. Lammertsma AA, Hume SP. Simplified reference tissue model for PET receptor studies. *Neuroimage* 1996; 4: 153–8.

24. Carne RP, Vogrin S, Litewka L, et al. Cerebral cortex: An MRI-based study of volume and variance with age and sex. *J Clin Neurosci* 2006; 13: 60–72.

25. Hirvonen J, Kajander J, Allonen T, et al. Measurement of serotonin 5-HT1A receptor binding using positron emission tomography and [carbonyl-(11)C]WAY-100635-considerations on the validity of cerebellum as a reference region. *J Cereb Blood Flow Metab* 2007; 27: 185–95.

26. Parsey RV et al. Higher Serotonin 1A Binding in a Second Major Depression Cohort: Modeling and Reference Region Considerations. *Biol Psychiatry* 2010; 68: 170–178.

27. Varnäs K, Halldin C, Hall H. Autoradiographic distribution of serotonin transporters and receptor subtypes in human brain. *Hum Brain Mapp* 2004; 22: 246–60.

28. Varnäs K, Hall H, Bonaventure P, et al. Autoradiographic mapping of 5-HT1B and 5-HT1D receptors in the post mortem human brain using [3H]GR 125743. *Brain Res* 2001; 915: 47–57.

29. Varnäs K, Nyberg S, Halldin C, et al. Quantitative analysis of [11C]AZ10419369 binding to 5-HT1B receptors in the human brain. *JCBFM* 2011; 31: 113–123.

30. Varnäs K, Nyberg S, Karlsson P, et al. Dose-dependent binding of AZD3783 to brain 5-HT1B receptors in non-human primates and human subjects: A positron emission tomography study with [11C]AZ10419369. *Psychopharmacology (Berl)* 2011; 213: 533–545.

31. Pazos A, Probst A, Palacios J. Serotonin receptors in the human brain—IV. Autoradiographic mapping of serotonin-2 receptors. *Neuroscience* 1987; 21: 123–139.

32. Hall H, Farde L, Halldin C, et al. Autoradiographic localization of 5-HT2A receptors in the human brain using M100907 and M100907. *Synapse* 2000; 431: 421–431.

33. Pinborg LH, Adams KH, Svarer C, et al. Quantification of 5-HT2A receptors in the human brain using [18F]altanserin-PET and the bolus/infusion approach. *J Cereb Blood Flow Metab* 2003; 23: 985–96.
34. Herth MM, Nymann I, Demant H, et al. Synthesis and evaluation of PET ligands F-labeled 5-HT 2A receptor agonists as. *Nucl Med Biol* 2016; 43: 455–462.
35. Leysen JE. 5-HT2 receptors. *Curr drug targets - CNS Neurol Disord* 2004; 3: 11–26.
36. Marazziti D, Rossi A. Distribution and characterization of mesulergine binding in human brain postmortem. *Eur ...* 1999; 10: 21–26.
37. Reynolds GP, Mason SL, Meldrum A, et al. 5-Hydroxytryptamine (5-HT)4 receptors in post mortem human brain tissue: distribution, pharmacology and effects of neurodegenerative diseases. *Br J Pharmacol* 1995; 114: 993–998.
38. Varnäs K, Halldin C, Pike V, et al. Distribution of 5-HT 4 receptors in the postmortem human brain—an autoradiographic study using SB 207710. *Eur ...* 2003; 13: 228–234.
39. Kish SJ, Furukawa Y, Chang L-J, et al. Regional distribution of serotonin transporter protein in postmortem human brain: is the cerebellum a SERT-free brain region? *Nucl Med Biol* 2005; 32: 123–8.
40. Parsey R V., Kent JM, Oquendo MA, et al. Acute Occupancy of Brain Serotonin Transporter by Sertraline as Measured by [11C]DASB and Positron Emission Tomography. *Biol Psychiatry* 2006; 59: 821–828.
41. Kent JM, Coplan JD, Lombardo I, et al. Occupancy of brain serotonin transporters during treatment with paroxetine in patients with social phobia: A positron emission tomography study with [11C]McN 5652. *Psychopharmacology (Berl)* 2002; 164: 341–348.
42. Shrestha S et al. Serotonin-1A receptors in major depression quantified using PET: controversies, confounds, and recommendations. *Neuroimage* 2012; 59: 3243–3251.
43. Eastwood SL, Burnet PWJ, Gittins R, et al. Expression of Serotonin 5-HT 2A Receptors in the Human Cerebellum and Alterations in Schizophrenia. 2001; 114: 104–114.

9 Figures

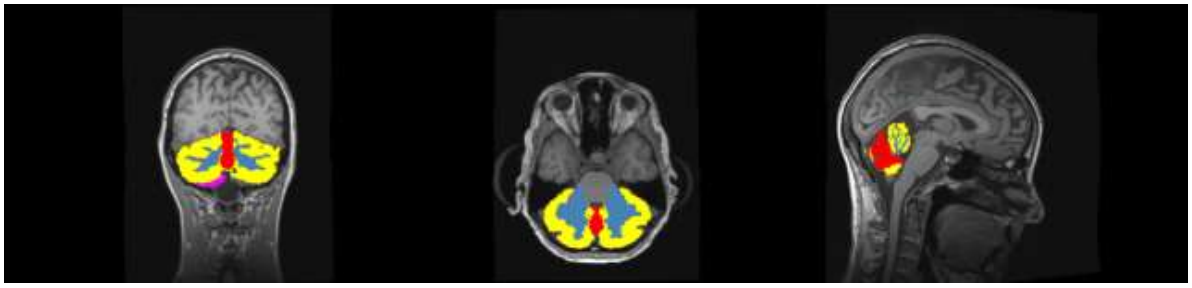

Figure 1.

The cerebellar hemispheres are segmented in CH (yellow) and cerebellar white matter (blue) by FreeSurfer, while CV is delineated along the midline with SUIT (red). The peripheral overlabeling by using outliers of the intersection of SUIT and FreeSurfer are shown in pink.

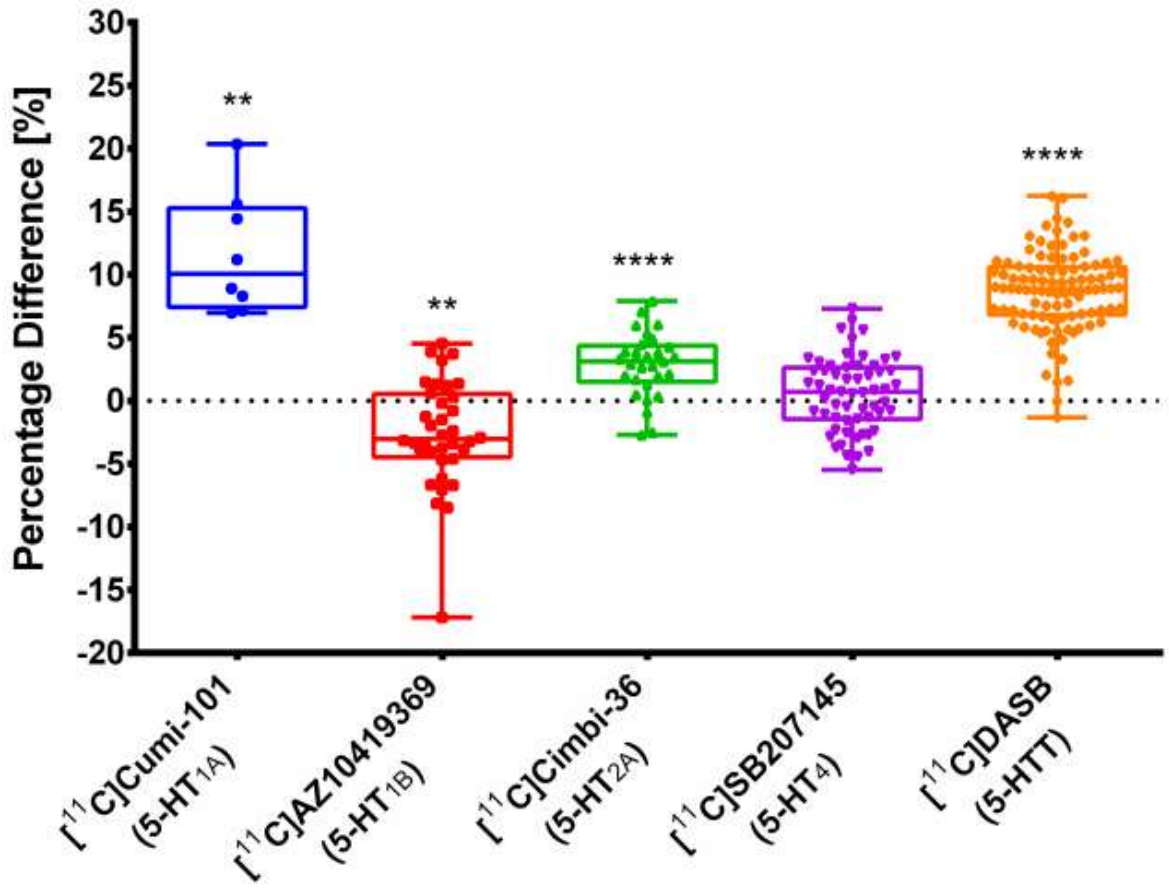

Figure 2. Percentage difference given as ($meanSUV_{CV}$-$meanSUV_{CH}$)/ $meanSUV_{CH}$ between mean SUV in CV and CH. The box plot displays the median as central line, the edges of the box are the 25th and 75th percentiles, the whiskers extend to the minimal and maximal data points, and all values are plotted as dots individually. Significance of within subjects, paired nonparametric two-sided Wilcoxon signed rank tests is given by *:p<0.05, **:p<0.01, ***:p<0.001, ****:p<0.0001.

.

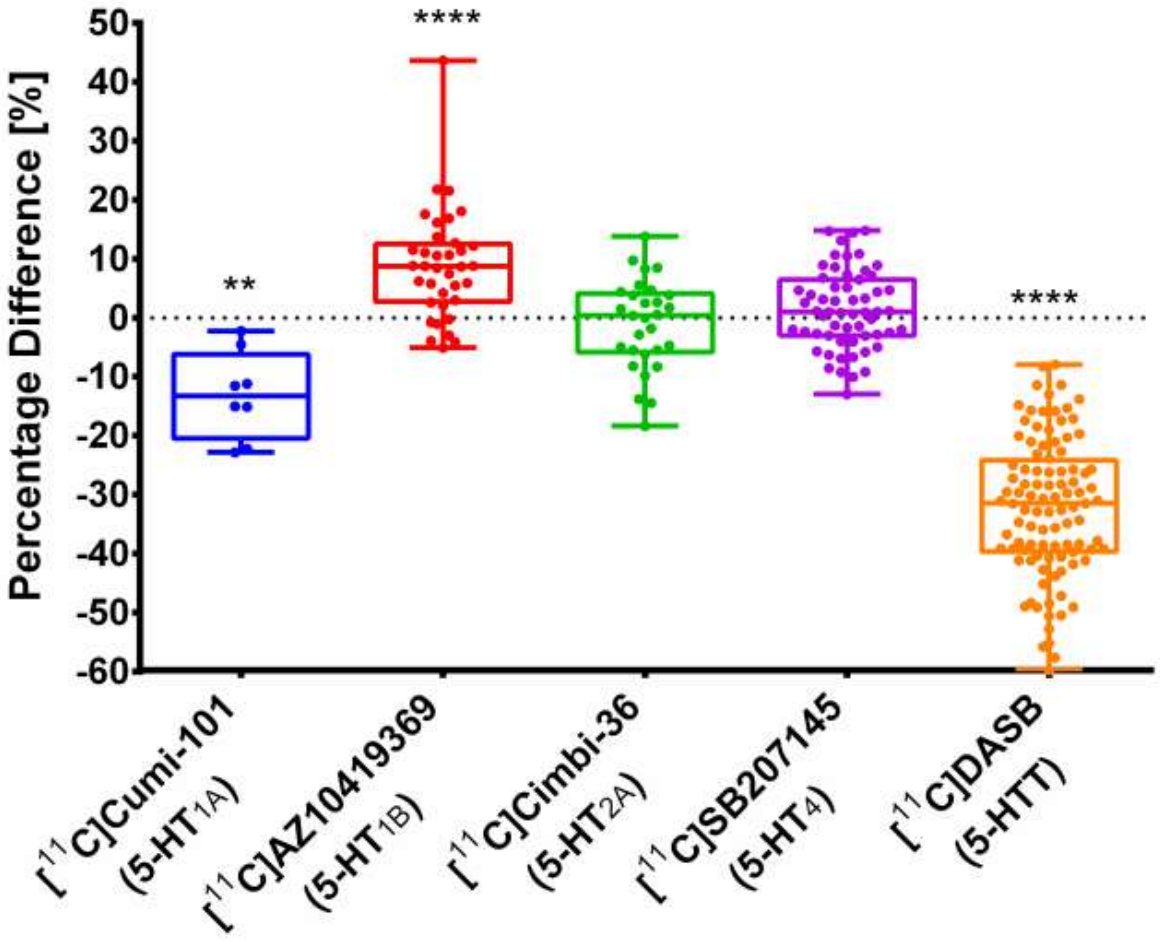

Figure 3. Percentage difference defined as ($BP_{ND,CV}$- $BP_{ND,CH}$)/ $BP_{ND,CH}$ in neocortical BP_{ND} calculated based on CV and CH. The box plot displays the median as central line, the edges of the box are the 25th and 75th percentiles, the whiskers extend to the minimal and maximal data points, and all values are plotted as dots individually. Significance of within subjects, paired nonparametric two-sided Wilcoxon signed rank tests is given by *:p<0.05, **:p<0.01, ***:p<0.001, ****:p<0.0001.

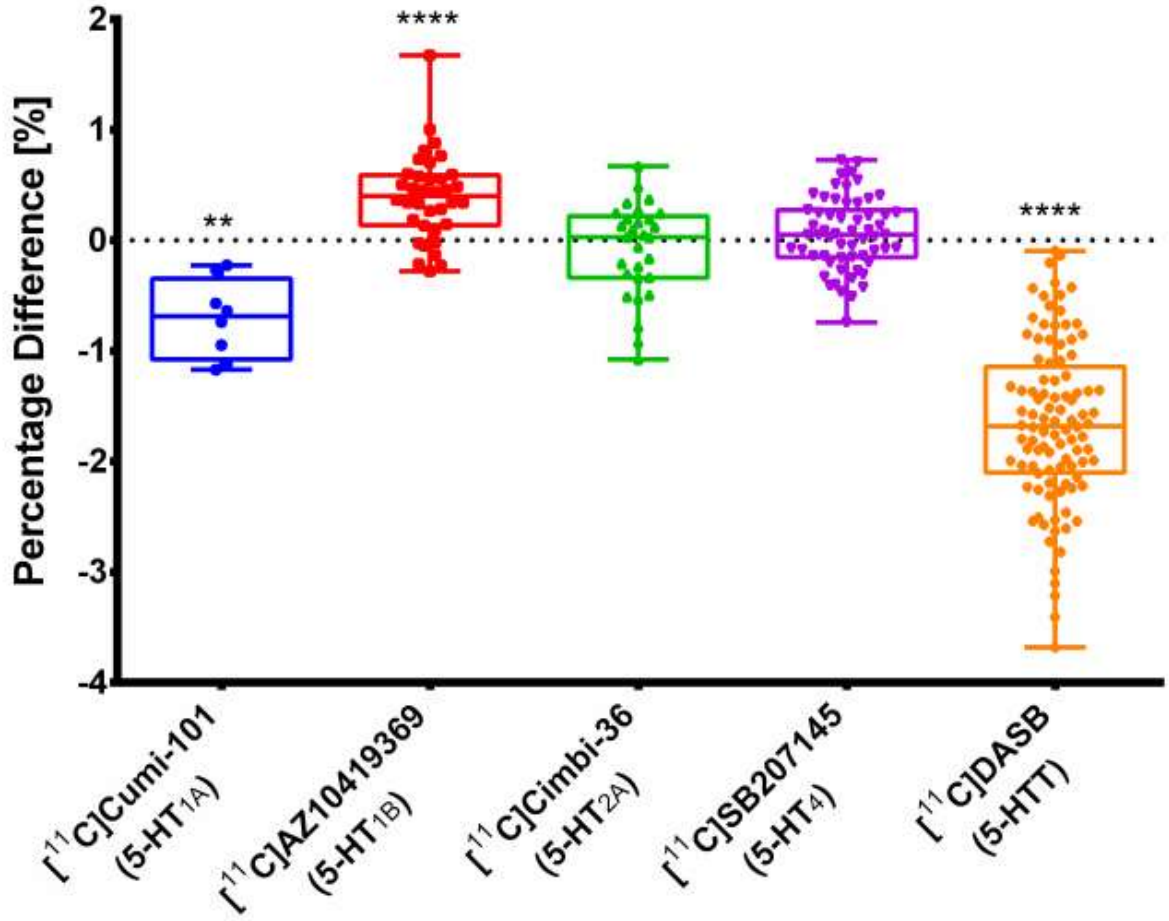

Figure 4. Percentage difference given as ($BP_{ND,CV+CH}$- $BP_{ND,CH}$)/ $BP_{ND,CH}$ in neocortical BP_{ND} calculated based on CV+CH and CH. The box plot displays the median as central line, the edges of the box are the 25th and 75th percentiles, the whiskers extend to the minimal and maximal data points, and all values are plotted as dots individually. Significance of within subjects, paired nonparametric two-sided Wilcoxon signed rank tests is given by *:p<0.05, **:p<0.01, ***:p<0.001, ****:p<0.0001.